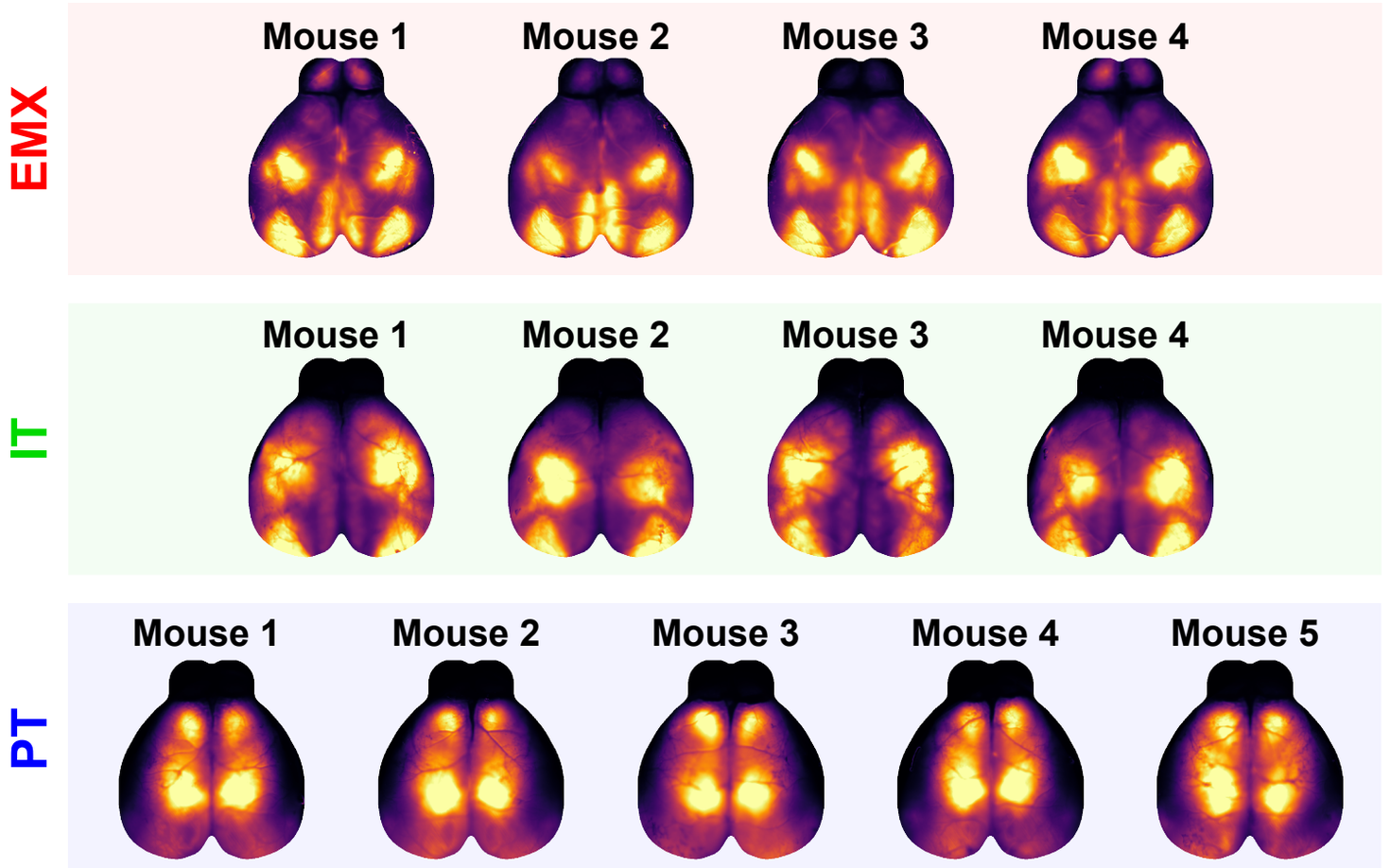

Supplementary Fig. 1. Cortical maps of total variance for individual mice
Maps of variance over all frames for individual mice in each PyN type group. Colors are normalized between zero and the 95th percentile for each animal. Distinct variance patterns for each PyN type were largely conserved across individual mice.

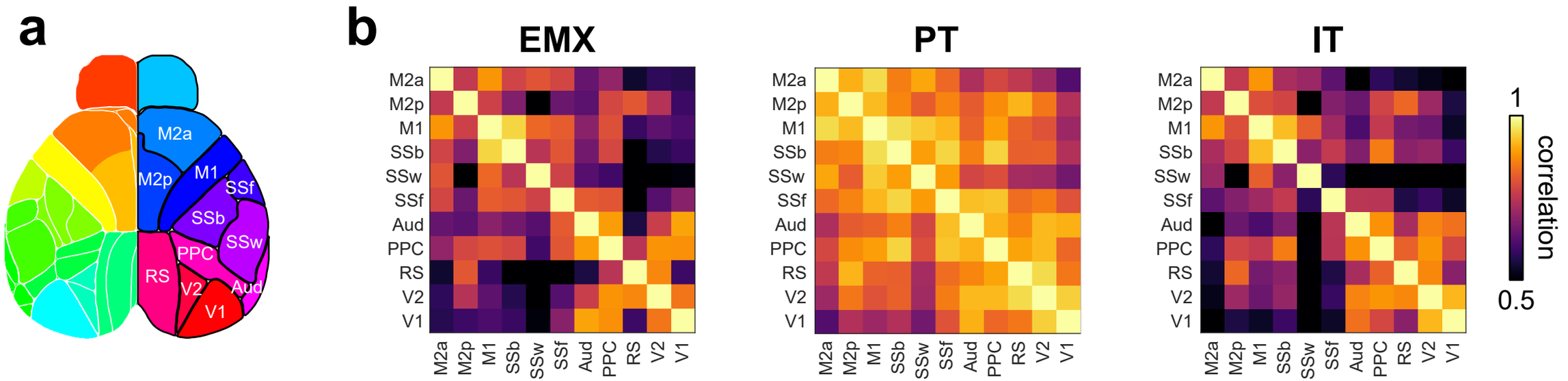

Supplementary Fig. 2. PyN-specific correlation patterns between cortical regions
a) Map of cortical regions, used for correlation analysis. V1 = primary visual cortex, V2 = secondary visual cortex, RS = retrosplenial cortex, Aud = auditory cortex, PPC = posterior parietal cortex, SSw = somatosensory whisker area, SSb = somatosensory body area, SSf = somatosensory face area, M1 = primary motor cortex, M2p = posterior secondary motor cortex, M2a = anterior secondary motor cortex. **b)** Correlations between cortical regions in EMX, PT and IT neurons averaged over all sessions and mice. Inter-region correlations were comparable between EMX and IT neurons but overall increased for PT neurons.

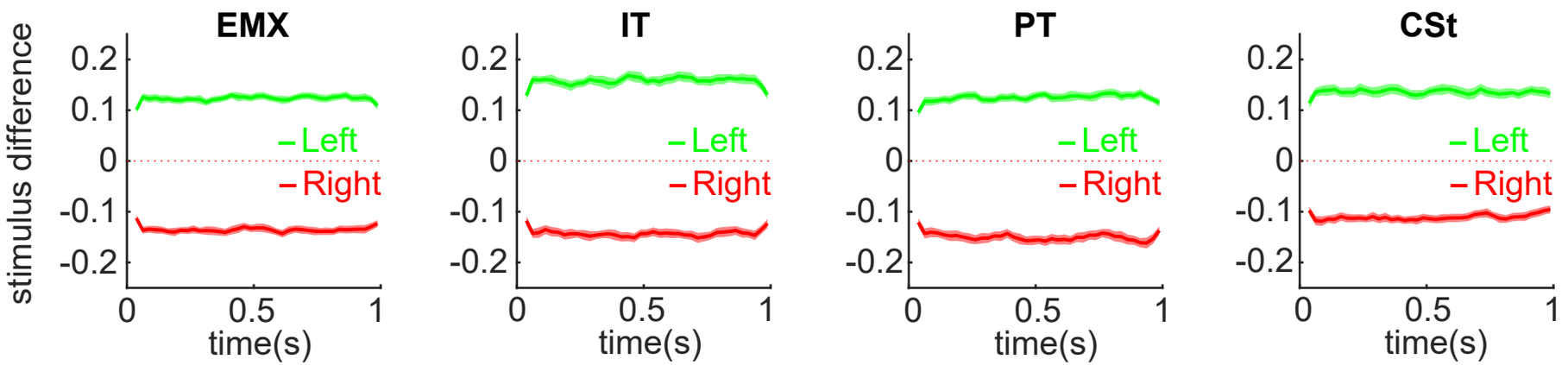

Supplementary Fig. 3. Mice in all PyN groups integrate sensory information throughout the stimulus period
Shown is the normalized difference between auditory clicks on the left or right side, when animals responded to the left (green) or the right (red). Binsize is 50 ms. Positive numbers indicate a higher probability of observing a leftward click sound, negative numbers indicate more clicks on the right. In all mice, the probability of observing more stimuli on the chosen side is consistently higher throughout the stimulus period. This shows that mice integrate sensory evidence from the entire stimulus period and individual click events have an equal influence animal decisions, regardless of their occurence early or late in the stimulus sequence.

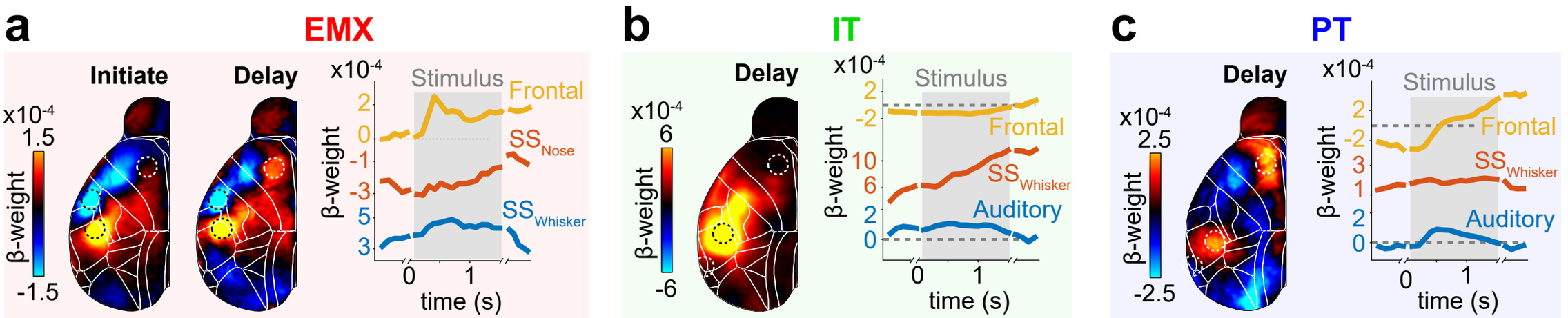

Supplementary Fig. 4. Choice-related activity in somatosensory cortex

a) Averaged choice kernel maps for EMX mice during initiation and delay periods. Dashed circles show the location of somatosensory whisker ($SS_{Whisker}$), somatosensory nose (SS_{Nose}), and frontal cortex. $SS_{Whisker}$ (blue trace) and SS_{Nose} (red trace) were constantly positive or negative, respectively, even during the initiation period. In contrast to frontal cortex (yellow trace), both areas were only weakly modulation by the stimulus onset (gray box). **b)** Choice kernel maps for IT mice during the delay period. Dashed circles show the location of auditory, $SS_{Whisker}$, and frontal cortex. Choice-related activity in $SS_{Whisker}$ (red trace) increased over the course of the trial. No choice-related modulation was observed in the frontal cortex. **c)** Choice kernel maps for PT mice during the delay period. Conventions as in b). Choice-related activity strongly increased in frontal crontal cortex after stimulus onset and was weaker in other cortical areas.

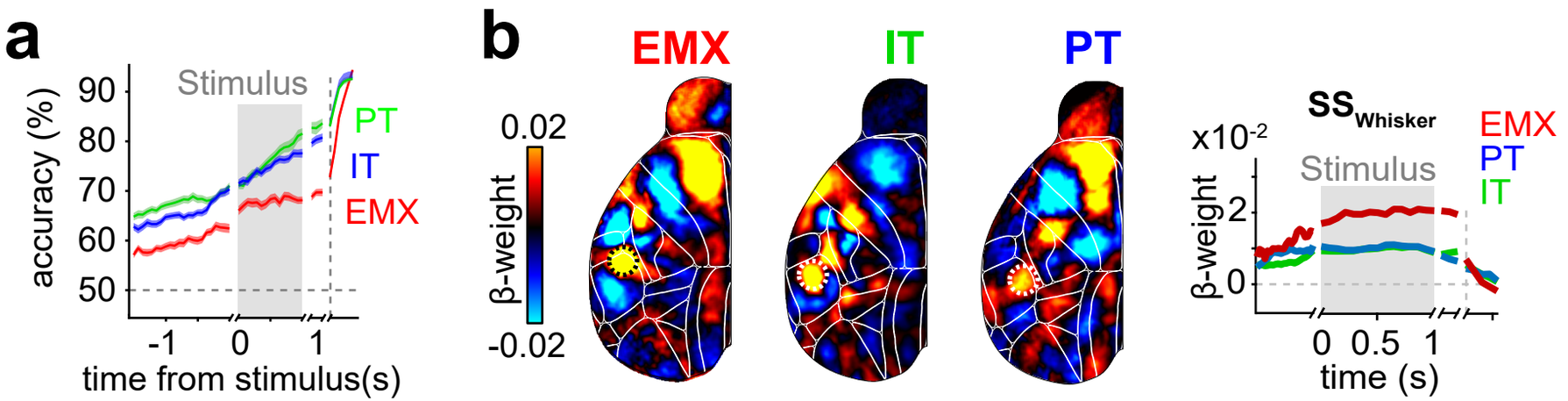

Supplementary Fig. 5. Choice decoder performance and choice signals in the somatosensory cortex

a) 10x cross-validated decoder performance, predicting an animal's left/right choices at different times during the trial. In all PyN types, decoder performance was above chance at all times, including the initiation period before the stimulus (gray box). This suggests that, in some trials, animals follow a pre-conceived choice that is stimulus-independent and can be decoded from cortical activity. Decoder performance was highest in the response period (dashed vertical line) when animals performed licking movements. **b)** Contralateral choice weight maps during the delay period (same as in Fig. 6c). Dashed circles show the location of somatosensory whisker cortex ($SS_{Whisker}$). In all PyN types, choice weights for $SS_{Whisker}$ increases during the initiation period before stimulus (gray box) onset. This indicates that pre-stimulus choices could be reflected in choice-specific whisker movements. Similar to choice kernels, we observed little modulation of choice signals in $SS_{Whisker}$ due to the stimulus onset.

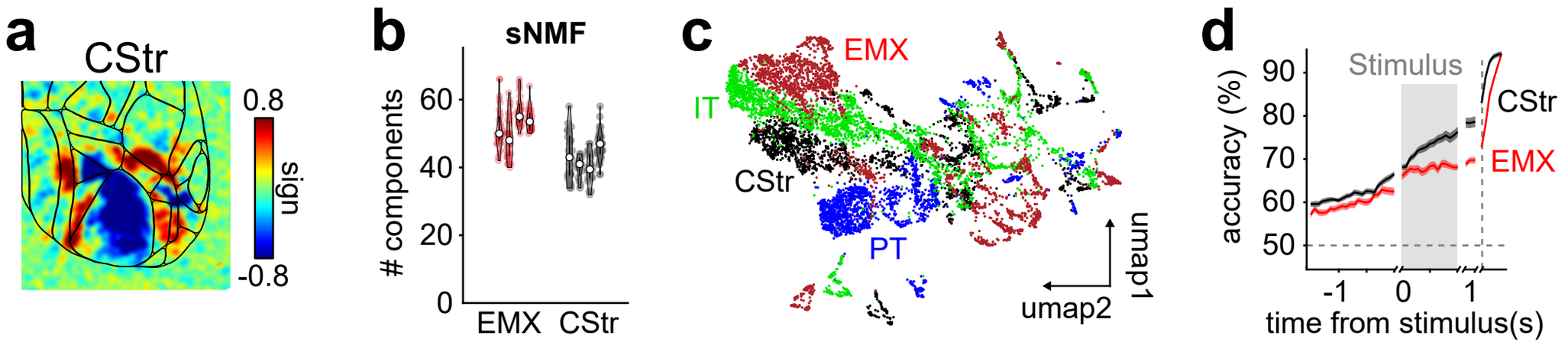

Supplementary Fig. 6. Retrograde labeling of CStr neurons reveals distinct cortical dynamics
a) Visual sign maps from retinotopic mapping. CStr neurons responded to visual stimulation and reveal comparable retinotopic organization as other PyN types. **b)** Number of sNMF components, accounting for 99% of cortical variance in EMX and CStr mice, data points represent individual sessions. CStr neurons required fewer components than EMX and IT but more components than PT neurons (compare with Fig. 2a). **c)** UMAP embedding of spatial sNMF components for EMX (red), IT (green), PT (blue) and CStr (black) mice. Data points show individual spatial components. CStr components were clearly distinct from other PyN types. **d)** Cross-validated choice-decoder accuracy. Decoder accuracy are shown for EMX (red) and CStr (black) neurons which continuously increased throughout the trial (gray region: stimulus period; dashed line: onset of response period).